

ORIGINAL ARTICLE

Long noncoding RNA *ANRIL* promotes the malignant progression of cholangiocarcinoma by epigenetically repressing *ERRF1* expression

Yang Yu¹ | Qiaoyu Chen²  | Xunlei Zhang¹ | Jian Yang³ | Kaibo Lin⁴ | Congfei Ji¹ | Aibing Xu¹ | Lei Yang¹ | Lin Miao⁵ 

¹Department of Oncology, Affiliated Tumor Hospital of Nantong University, Nantong, China

²Department of Pathology, Zhejiang University School of Medicine Second Affiliated Hospital, Hangzhou, China

³Department of Urology, Second Affiliated Hospital of Nanjing Medical University, Nanjing, China

⁴Department of Assisted Reproduction, Shanghai Ninth Hospital, Shanghai Jiao Tong University, Shanghai, China

⁵Medical Centre for Digestive Diseases, Second Affiliated Hospital of Nanjing Medical University, Nanjing, China

Correspondence

Lei Yang, Department of Oncology, Affiliated Tumor Hospital of Nantong University, Nantong, Jiangsu, China.
Email: leiyang.53@163.com

Lin Miao, Medical Centre for Digestive Diseases, Second Affiliated Hospital of Nanjing Medical University, Nanjing, Jiangsu, China.
Email: linmiao@njmu.edu.cn

Funding information

Project of the peak of the six talents of Jiangsu Province, Grant/Award Number: WSN-018; Scientific Research Foundation for Health of Jiangsu Province, Grant/Award Number: H201408; Project of Standard Diagnosis and Treatment of Key Disease of Jiangsu Province, Grant/Award Number: BE2015722

Abstract

Long noncoding RNAs (lncRNAs) have recently been verified to have significant regulatory functions in many types of human cancers. The lncRNA *ANRIL* is transcribed from the *INK4b-ARF-INK4a* gene cluster in the opposite direction. Whether *ANRIL* can act as an oncogenic molecule in cholangiocarcinoma (CCA) remains unknown. Our data show that *ANRIL* knockdown greatly inhibited CCA cell proliferation and migration in vitro and in vivo. According to the results of RNA sequencing analysis, *ANRIL* knockdown dramatically altered target genes associated with the cell cycle, cell proliferation, and apoptosis. By binding to a component of the epigenetic modification complex enhancer of zeste homolog 2 (EZH2), *ANRIL* could maintain lysine residue 27 of histone 3 (H3K27me3) levels in the promoter of ERBB receptor feedback inhibitor 1 (*ERRF1*), which is a tumor suppressor gene in CCA. In this way, *ERRF1* expression was suppressed in CCA cells. These data verified the key role of the epigenetic regulation of *ANRIL* in CCA oncogenesis and indicate its potential as a target for CCA intervention.

KEYWORDS

ANRIL, cholangiocarcinoma, epigenetic regulation, *ERRF1*, long noncoding RNA

Abbreviations: ASO, antisense oligonucleotide; CCA, cholangiocarcinoma; *ERRF1*, ERBB receptor feedback inhibitor 1; EZH2, enhancer of zeste homolog 2; H3K27me3, lysine residue 27 of histone 3; lncRNA, long noncoding RNA; qRT-PCR, quantitative RT-PCR; RNA-seq, RNA sequencing; si-SC, scrambled negative control siRNA; SPRY4, sprouty RTK signaling antagonist 4; TCGA, The Cancer Genome Atlas.

Yang Yu, Qiaoyu Chen, Xunlei Zhang, and Jian Yang equal contributors.

This is an open access article under the terms of the Creative Commons Attribution-NonCommercial-NoDerivs License, which permits use and distribution in any medium, provided the original work is properly cited, the use is non-commercial and no modifications or adaptations are made.

© 2020 The Authors. *Cancer Science* published by John Wiley & Sons Australia, Ltd on behalf of Japanese Cancer Association.

1 | INTRODUCTION

Cholangiocarcinoma, the most frequently occurring biliary tract cancer, accounts for 3% of all gastrointestinal malignancies and originates from the ductal epithelial cells lining the intrahepatic and extrahepatic biliary ducts.^{1,2} Cholangiocarcinoma is a destructive malignancy with an extreme overall 5-year survival rate of less than 10%.³ These patients have a median survival of 24 months after diagnosis, which indicates that CCA has a poor prognosis.⁴ Although surgical resection and liver transplantation are possible curative treatment choices for early-stage CCA patients, the median 5-year survival after R0 resection is approximately 30%.⁵ However, because of the destructive nature of CCA, most patients already have advanced disease at diagnosis.³ What is more, patients with CCA are insensitive to conventional chemotherapy or radiotherapy.⁶ Therefore, there are no potentially curative clinical therapeutic interventions for CCA, and no targeted molecular therapies have been adopted for use in CCA.

Long noncoding RNAs are over 200 nucleotides in length and represent an enormous RNA family. Long noncoding RNAs have limited protein coding potential and lack detectable ORFs, which are necessary for protein coding potential.⁷⁻¹¹ Recently, lncRNAs have been reported to serve as pivotal regulators in many biological processes, such as cellular proliferation, development, and differentiation. Long noncoding RNAs can alter the expression of genes involved in diverse biological functions¹² by binding to transcription factors,¹³ chromatin-modifying factors,¹⁴⁻¹⁶ or heterogeneous nuclear ribonucleoproteins.¹⁷ Long noncoding RNAs can act as regulators of the alternative splicing, translation, or stability of host mRNAs by posttranscriptional mechanisms; they can also serve as scaffolds or guides to regulate protein-protein or protein-DNA interactions^{18,19} and can act as endogenous microRNA sponges to modulate microRNA targets.²⁰⁻²² Notably, abnormal lncRNA expression has been proven in many cancers, including CCA.²³⁻³⁰

Among them, the lncRNA *ANRIL* (CDKN2B antisense RNA 1), which is transcribed from the *INK4b-ARF-INK4a* gene cluster in the opposite direction, has been identified as a shared genetic susceptibility locus associated with intracranial aneurysm,^{31,32} coronary disease,³³ and various types of cancer. In particular, this susceptibility locus has been associated with the invasive pathophysiology of ovarian cancer,³⁴ nasopharyngeal carcinoma,³⁵ hepatocellular carcinoma,³⁶ lung cancer,^{37,38} epithelial ovarian cancer,³⁴ colorectal cancer,^{39,40} cervical cancer,⁴¹ and gastric cancer.⁴² Regarding the underlying molecular mechanism, *ANRIL* can be induced by the ATM-E2F1 signaling pathway⁴³ and is required for silencing the *p15(INK4B)* tumor suppressor gene.⁴⁴ In non-small cell lung cancer, *ANRIL* promotes non-small cell lung cancer cell proliferation and inhibits apoptosis by silencing *KLF2* and *P21* expression by binding to PRC2.³⁸ In hepatocellular carcinoma, *ANRIL* regulates cell apoptosis by epigenetically silencing *KLF2*.³⁸

We speculated that many lncRNAs remain unexplored in CCA, particularly those with dysfunctional expression patterns. To comprehensively characterize aberrantly expressed lncRNAs in CCA, we analyzed TCGA CCA and normal tissue RNA sequencing data (9 normal and 36 cancer samples) and 1 independent microarray dataset from

the Gene Expression Omnibus database (GSE76297; 92 cancer tissue samples and 91 normal tissue samples). We discovered a CCA-specific upregulated lncRNA termed *ANRIL* that was expressed at higher levels in CCA tissues than in normal tissues. The functional association between the underlying molecular mechanism and *ANRIL* overexpression in CCA had not been determined. Our data showed that *ANRIL* knockdown greatly inhibited CCA cell proliferation and migration in vitro and in vivo. According to the RNA-seq analysis results, *ANRIL* knockdown dramatically altered target genes associated with the cell cycle, cell proliferation, and apoptosis. By binding to a component of EZH2, *ANRIL* could maintain H3K27me3 levels in the promoter of *ERRF1*, which was verified to act as a tumor suppressor gene in CCA. In this way, *ANRIL* expression was suppressed in CCA cells. These data verified the key role of the epigenetic regulation of the lncRNA *ANRIL* in CCA oncogenesis and indicate its potential as a target for CCA intervention.

2 | MATERIALS AND METHODS

2.1 | Tissue collection and ethics statement

A total of 17 samples were collected during resection for CCA at the Second Affiliated Hospital of Nanjing Medical University. After removal, all specimens were instantly frozen in tubes with RNAlater and stored in liquid nitrogen until RNA extraction. Our research was approved by the Ethics Committee of Nanjing Medical University, and written consent was obtained from every patient.

2.2 | RNA extraction and qRT-PCR analyses

All RNA was obtained from cultured cells or specimens with TRIzol reagent (Invitrogen). For RT-qPCR, 1 μ g RNA was reverse transcribed into cDNA with a Reverse Transcription Kit (Takara). Real-time PCR analyses were carried out with SYBR Green (Takara). The findings were normalized to the expression of GAPDH. The primer sequences are shown in Table S1.

2.3 | Cell culture

The CCA cell lines HuCCT1 and RBE were obtained from the Institute of Biochemistry and Cell Biology of the Chinese Academy of Sciences (Shanghai, China). All cell lines were maintained in DMEM (Life Technologies) with 10% FBS (Sciencell), 100 mg/mL streptomycin, and 100 U/mL penicillin (Invitrogen) in humidified air at 37°C with 5% CO₂.

2.4 | Cell line transfection

Cholangiocarcinoma cells were plated in 6-well plates and transfected the next day with particular siRNAs (100 nmol/L) or si-SC

(100 nmol/L; Invitrogen) using Lipofectamine 2000 (Invitrogen) according to the manufacturer's protocol. A lentiviral shRNA vector targeting *ANRIL* was generated by inserting stand oligonucleotides into the pENTR/CMV/U6 vector, HuCCT1 cells were infected with the sh-*ANRIL* vectors and selected with puromycin (5 µg/mL) to establish stable shRNA-*ANRIL* cell lines. The siRNA and shRNA sequences are shown in Table S1.

2.5 | Subcellular fractionation

Nuclear and cytosolic fractions were separated with a PARIS Kit (Life Technologies) according to the manufacturer's instructions.

2.6 | Cell proliferation analysis

Cell viability was determined with CCK-8 assays according to the manufacturer's suggestions. HuCCT1 and RBE cells transfected with siRNA or si-SC (3000 cells/well) were cultivated in 5 96-well plates with 6 replicate wells. For the colony formation assays, 500 transfected cells were plated in a 6-well plate and maintained in media with 10% FBS for 2 weeks. The medium was replaced every 4 days. Then colonies were treated with methanol and dyed with a 0.1% crystal violet solution (Sigma-Aldrich) for 15 minutes. The number of visibly stained colonies was counted for colony formation. The wells were independently measured in triplicate for the different treatment groups.

2.7 | Cell migration assays

For the migration assays, after 24 hours of transfection, 3.5×10^4 cells in media with 1% FBS were put into the upper chamber of an insert (Millipore), and medium with 10% FBS was put into the lower chamber. After 24 hours of incubation, the remaining cells on the upper layer of the membrane were removed, while those cells that had migrated through the membrane were dyed with methanol and a 0.1% crystal violet solution and imaged with an IX71 inverted microscope (Olympus). This experiment was carried out in triplicate.

2.8 | Flow cytometric analysis

Flow cytometry assays were carried out as previously reported in Xu et al.⁴⁵ After the cells were transfected with siRNAs for 48 hours, we harvested the cells and then undertook FITC-annexin V and propidium iodide staining using an FITC-annexin V Apoptosis Detection Kit (BD Biosciences) according to the manufacturer's instructions. Cell cycle analysis was determined by propidium iodide staining using a CycleTest Plus DNA Reagent Kit (BD Biosciences) according to the manual. The results were evaluated with a FACScan flow cytometer. The numbers of cells in each phase were assessed.

2.9 | Western blot assay and Abs

Cell protein lysates were separated by 10% SDS-PAGE and transferred onto 0.22-µm nitrocellulose blotting membranes (Sigma-Aldrich). The membranes were incubated with the indicated Abs. Densitometry (Quantity One software; Bio-Rad) was used to quantify the autoradiograms. A GAPDH Ab was used as a control. An anti-EZH2 Ab was purchased from Proteintech, and an anti-*ERRF1* Ab was purchased from Genetex.

2.10 | In vivo tumor formation assay

Four-week-old athymic male mice from the Animal Center of Nanjing University (Nanjing, China) were kept in specific pathogen-free conditions. HuCCT1 cells were stably transfected with shRNA or empty vector and harvested from cell culture plates. The cells were then washed with PBS and resuspended at 2×10^7 cells/mL. Next, these cells were xenografted into BALB/c male nude mice. The tumor sizes were measured every 3 days, and the volumes were calculated as follows: length \times width² \times 0.5. At 16 days postinjection, the mice were subjected to CO₂ asphyxiation, and the tumors were weighed and examined. The study was carried out strictly in accordance with the Guidelines for the Care and Use of Laboratory Animals of the NIH. The protocol was approved by the Committee on the Ethics of Animal Experiments of Nanjing Medical University.

2.11 | RNA immunoprecipitation assays

To study whether *ANRIL* could interact with EZH2, we undertook a RIP experiment with a Magna RIP RNA-Binding Protein Immunoprecipitation Kit (Millipore) following the manufacturer's instructions. The Ab used for the EZH2 RIP assays was obtained from Millipore (Cat. #17-662).

2.12 | Chromatin immunoprecipitation assays

The ChIP assays were carried out with an EZ-ChIP Kit according to the manufacturer's recommendations (Millipore). EZH2 Abs (Cat. #17-662) and H3K27me3 Abs (Cat. # 07-449) were purchased from Millipore. The sequences of the ChIP primers are shown in Table S1. The equation used for calculating the ChIP data as a proportion relative to the DNA input was as follows: $2(\text{Input Ct} - \text{Target Ct}) \times 0.1 \times 100$.

2.13 | Deep sequencing of the whole transcriptome

Total RNA from *ANRIL* knockdown and control HuCCT1 cells was separated and quantified. The concentrations for each specimen were measured with a NanoDrop 2000 (Thermo Scientific) and evaluated with an Agilent2200 (Agilent). The sequence library for

each RNA specimen was created with an Ion Proton Total RNA-Seq Kit version 2 according to the manufacturer's instructions (Life Technologies). The data are shown in Table S2.

2.14 | Statistical analysis

Statistical analyses were carried out with GraphPad Prism 5 (GraphPad Software). The statistical significance of differences between various groups was calculated by Student's *t* test or the χ^2 test as appropriate. All data are expressed as the means \pm SD, and 2-sided *P* values of .05 were used to indicate statistical significance.

3 | RESULTS

3.1 | ANRIL is upregulated in human CCA tissues

To comprehensively characterize aberrantly expressed lncRNAs in CCA, we analyzed TCGA CCA and normal tissue RNA sequencing data (9 normal and 36 cancer samples) (Figure 1A) and 1 independent microarray dataset from the Gene Expression Omnibus database (GSE76297; 92 cancer tissue samples and 91 normal tissue samples)

(Figure 1B). The results showed that *ANRIL* was differentially expressed in CCA tissues and normal tissues (*P* value = 9.95×10^{-5}), which provided a clue for our research. *ANRIL*, a 3857 nt lncRNA, is transcribed from the antisense strand of the *INK4A-ARF-INK4B* gene, which was overexpressed in many other cancers, such as prostate cancer,⁴⁶ cervical cancer,⁴¹ and breast cancer,⁴⁷ so we wanted to validate whether it is also important in CCA. To further verify the informatics data, we detected *ANRIL* expression in a cohort of 17 paired CCA tumors and adjacent tissues by qRT-PCR. The results confirmed that *ANRIL* expression was remarkably higher in carcinoma tissues than in normal tissues (Figure 1C). Our data indicated that upregulated *ANRIL* expression is related to human CCA.

3.2 | ANRIL knockdown in CCA cell lines inhibits cell proliferation and migration

We first investigated the effects of increased *ANRIL* expression in CCA. The qRT-PCR results showed that *ANRIL* expression was significantly lower in the siRNA-mediated knockdown group than in the si-SC group for the HuCCT1 and RBE cell lines (Figure 2A). Both siRNA and ASO are interference technologies of lncRNA.^{48,49} Although it is possible that ASO has a better interference efficiency

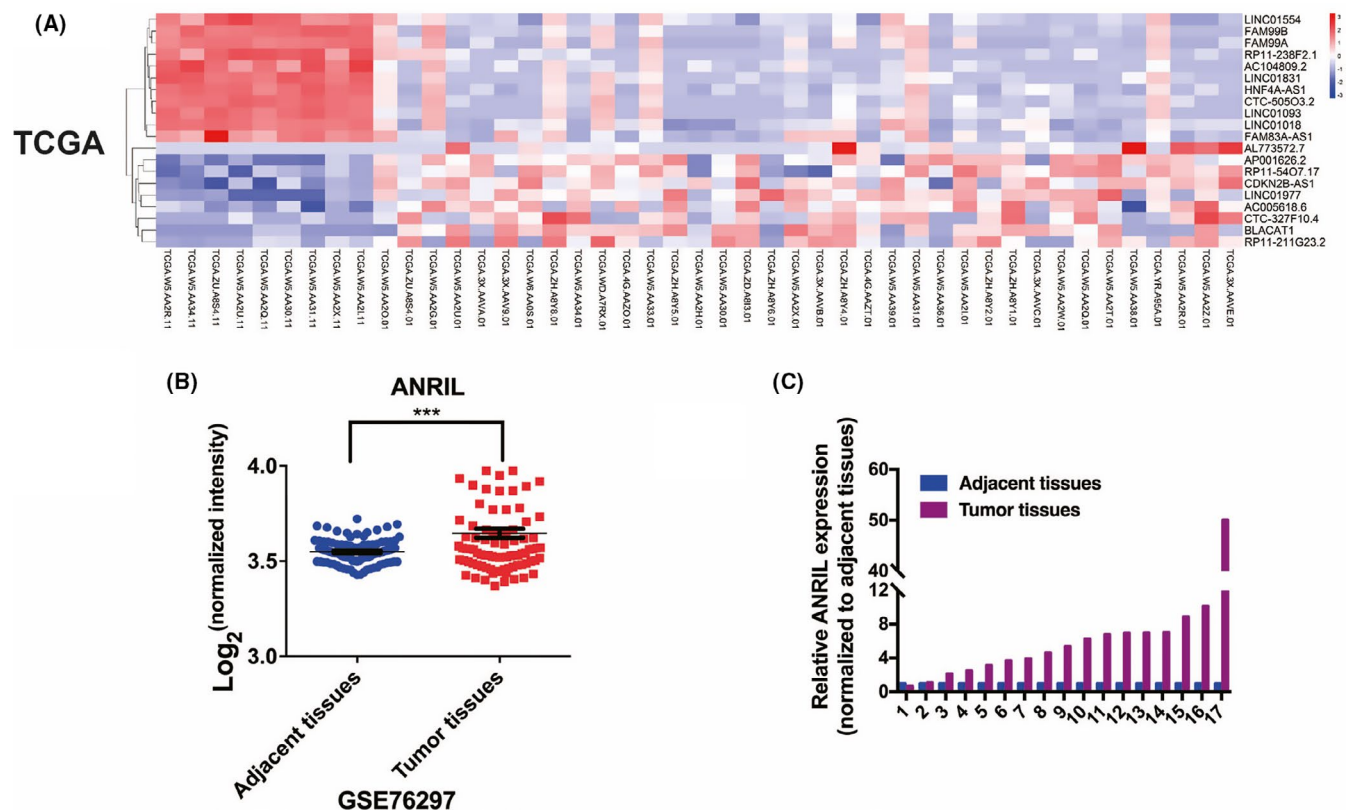


FIGURE 1 Increased long noncoding RNA (lncRNA) *ANRIL* levels in cholangiocarcinoma (CCA) tissues. A, Hierarchical clustering analysis of lncRNAs that were differentially expressed (*P* < .05) in CCA tissues and normal tissues from The Cancer Genome Atlas (TCGA) database. B, *ANRIL* was overexpressed in Gene Expression Omnibus datasets (GSE76297). C, *ANRIL* was detected in 17 pairs of CCA tissues by quantitative RT-PCR. *ANRIL* levels are significantly higher in CCA tissues than in nontumorous tissues. Error bars indicate means \pm SD.

****P* < .001

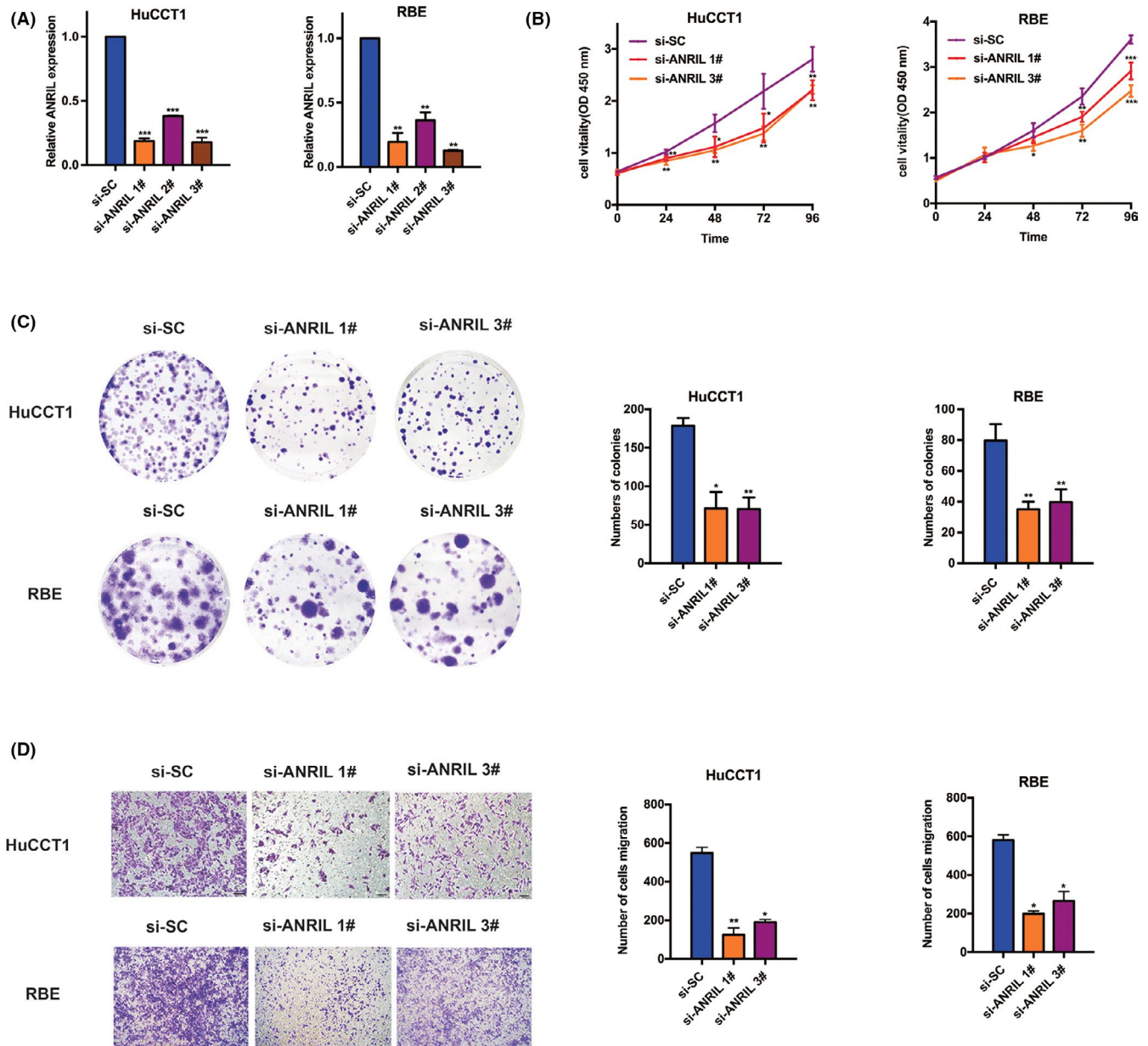


FIGURE 2 *ANRIL* promotes cell proliferation and migration in cholangiocarcinoma (CCA) cells. A, Quantitative RT-PCR was used to detect *ANRIL* expression in HuCCT1 and RBE cell lines after siRNA transfection. B, CCK-8 assays were used to determine cell viability in si-*ANRIL*-transfected CCA cells. C, Colony formation assays were used to determine the cell colony formation ability of si-*ANRIL*-transfected cells. D, Transwell assays showed that *ANRIL* knockdown inhibits CCA cell migration. Error bars indicate means \pm SD. * $P < .05$, ** $P < .01$; *** $P < .001$. si-SC, scrambled negative control siRNA

for lncRNA in the nucleus than siRNA, qPCR detection after siRNA interference showed that siRNA could efficiently inhibit the expression of *ANRIL*. Therefore, siRNA was used for interference in this project. The CCK-8 assays revealed that, compared to control cells, *ANRIL* knockdown cells had significantly lower cell viability for both the HuCCT1 and RBE cell lines (Figure 2B). Additionally, the clonogenic formation number was significantly lower in the *ANRIL* knockdown cells than in the 2 CCA cell lines (Figure 2C). Furthermore, Transwell assays showed that *ANRIL* knockdown dramatically repressed the migration of cells (Figure 2D). These data showed that *ANRIL* plays a vital role in CCA cell proliferation and migration.

3.3 | *ANRIL* depletion leads to increased cell apoptosis and delayed cell cycle in CCA cell lines

To further study whether *ANRIL* could affect apoptosis in CCA cell lines, flow cytometry was carried out. The findings revealed that HuCCT1 and RBE cell lines transfected with *ANRIL* siRNA showed higher apoptotic rates than the control cells (Figure 3A). Next, to determine whether the effects of *ANRIL* on CCA cell proliferation and apoptosis are caused by *ANRIL*-mediated alterations to cell cycle progression, we undertook flow cytometry assays for both HuCCT1 and RBE cell lines. The flow cytometry assays revealed that the numbers

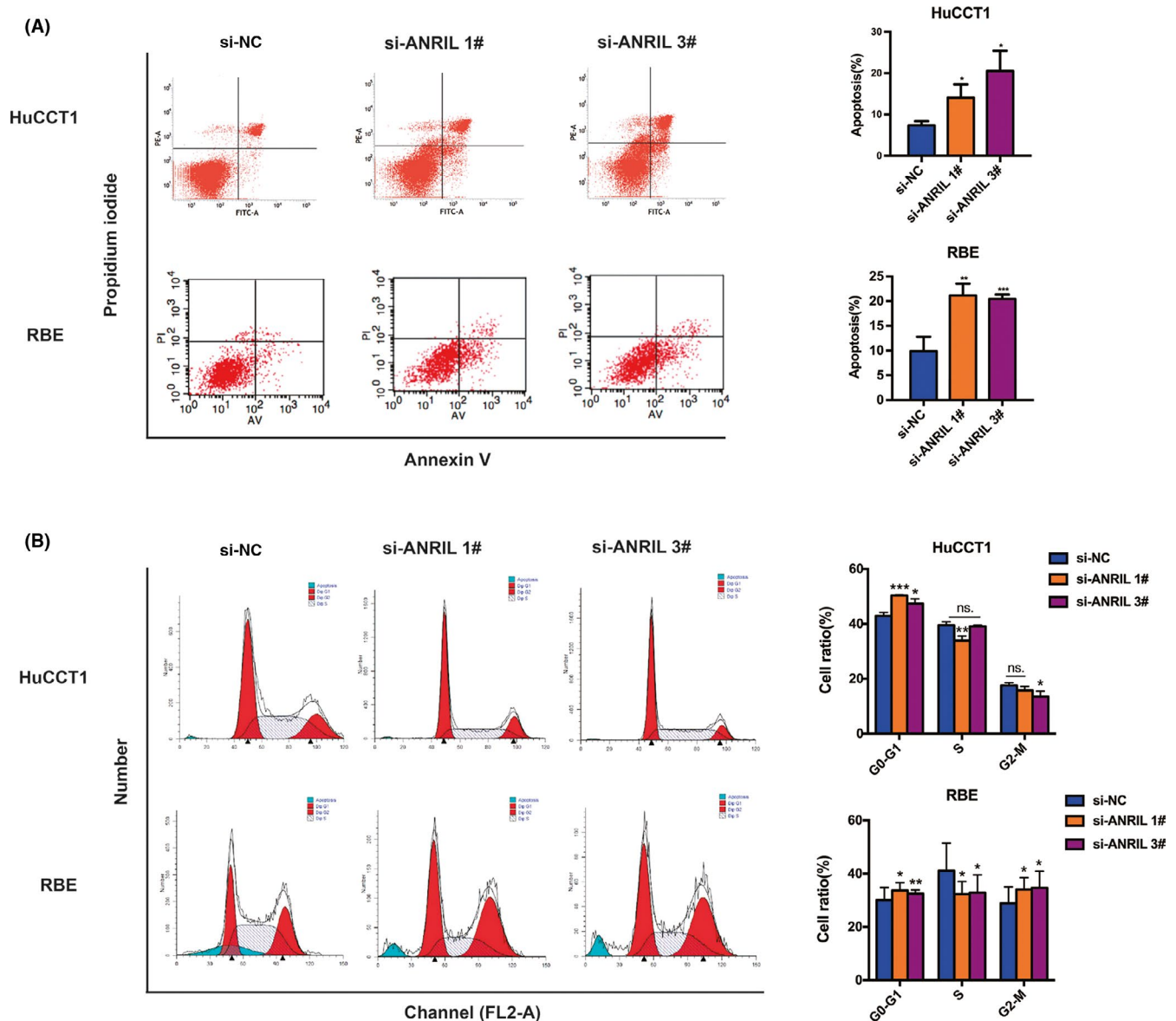


FIGURE 3 ANRIL depletion increases cell apoptosis and delays the cell cycle in cholangiocarcinoma (CCA) cell lines. A, FACS analysis of the effect of ANRIL on cell apoptosis. B, FACS analysis of the effect of ANRIL on cell cycle progression. Error bars indicate means \pm SD. * $P < .05$, ** $P < .01$; *** $P < .001$; n.s., not significant; si-NC, negative control siRNA; si-SC, scrambled negative control siRNA

of cells in the G₀/G₁ phase were higher and that the numbers of cells in the S and G₂/M phases were lower in ANRIL knockdown cells than in control cells (Figure 3B). Thus, ANRIL could accelerate cell proliferation, inhibit apoptosis, and regulate cell cycle progression in CCA cell lines.

3.4 | ANRIL knockdown inhibits CCA cell tumorigenesis in vivo

To determine whether ANRIL influences CCA tumorigenesis in vivo, HuCCT1 cells transfected with sh-ANRIL or control vector were injected into nude mice. At 16 days postinjection, the tumors established in the sh-ANRIL group were dramatically smaller than those in the control group (Figure 4A,B). Correspondingly, the average tumor

volumes and weights at the final time point were obviously lower in the sh-ANRIL group than in the control vector group (Figure 4C,D). Our results showed that silencing ANRIL could repress CCA tumor growth in vivo, indicating that the lncRNA ANRIL plays a significant role in CCA tumor growth.

3.5 | Cell proliferation and apoptosis pathways altered by ANRIL siRNAs

To determine the target genes that could be regulated by ANRIL in CCA, RNA transcriptome sequencing was carried out using control and siRNAs against ANRIL. A set of 1383 mRNAs had a minimum of 1.5-fold increase in abundance, whereas 1350 genes had a decrease in abundance (less than 1.5-fold) after ANRIL silencing (Figure 5A,

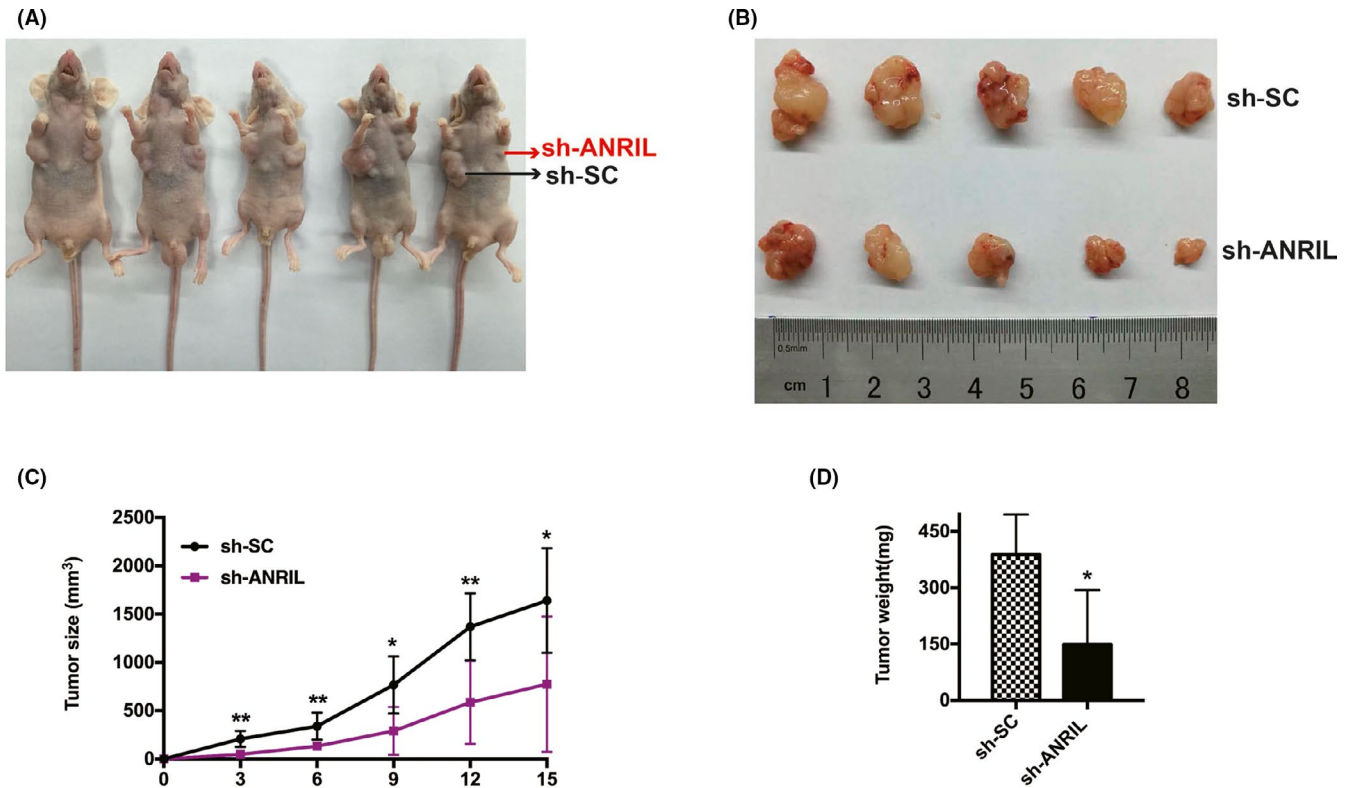


FIGURE 4 ANRIL promotes cholangiocarcinoma cell tumor growth in vivo. A, B, Scrambled (sh-SC) or sh-ANRIL was stably transfected into HuCCT1 cells, which were then injected into nude mice. C, Tumor volumes were calculated every 4 days after injection. Bars indicate SD. D, Tumor weights represent means \pm SD * $P < .05$; ** $P < .01$

Table S2). An in-depth investigation of the gene ontology analysis indicated that the most markedly overrepresented biological process pathways involved the cell cycle, cell proliferation, and cell apoptosis (Figure 5B). To prioritize the most strongly ANRIL-related genes, attention was paid to those most highly expressed following ANRIL knockdown. Prospectively, among the most highly expressed genes, many well-known genes related to proliferation and migration (eg *PTPRH*, *CXCL2*, *GOS2*, *ERRF1*, *GDF15*, *ANGPTL4*, and *SPRY4*) were included. Some of these genes were verified by qRT-PCR after ANRIL knockdown in HuCCT1 and RBE cells (Figure 5C,D).

3.6 | ANRIL epigenetically silenced *ERRF1* transcription through EZH2-mediated H3K27me3 demethylation

Recent studies have reported that many lncRNAs cooperate with chromatin-modifying enzymes to accelerate epigenetic activation and thus silence target gene expression.⁵⁰ In particular, PRC2, a classical methyltransferase that comprises EZH2, EED, and SUZ12, can serve as a catalyst in both the dimethylation and trimethylation of H3K27me3 to epigenetically repress target gene expression.^{51,52} In our study, to investigate the mechanism of ANRIL-mediated regulation, we first carried out subcellular fractionation location assays, which verified ANRIL localization to mainly the nucleus (Figure 6A). In addition, the probability of interaction between EZH2 and ANRIL

was predicted on the RNA-Protein Interaction Prediction website, and the result showed that EZH2 could bind well with ANRIL (random forest = 0.7, support vector machine = 0.97) (<http://priddb.gdcbi.ia.sta.te.edu/RPISeq/index.html>) (Figure 6B). As revealed in Figure 6C, endogenous ANRIL was amplified in the anti-EZH2 RIP fraction relative to the input; the IgG fraction of HuCCT1 and RBE cell lines with an Ab against enhancer of EZH2 was used for comparison. Taken together, these results confirmed that ANRIL could interact with EZH2.

Subsequently, we hypothesized that EZH2 could coregulate the suppression of these ANRIL-mediated genes by binding with ANRIL. We first investigated the expression of ANRIL-suppressed genes with EZH2 absent or present using qRT-PCR. The results showed that the ANRIL-suppressed genes were increased by also knocking down EZH2 (Figure 6D,E) in HuCCT1 and RBE cell lines. Subsequently, a correlation analysis of the GSE76297 dataset (92 pairs of cancer and 91 normal tissue samples) from the Molecular Signature Database revealed that *ERRF1* was significantly negatively correlated with EZH2 (Figure 6F). Moreover, *ERRF1* protein levels were increased by knocking down EZH2 (Figure 6G) and ANRIL (Figure 6H). To further determine whether ANRIL suppressed the expression of *ERRF1* by interacting with EZH2, a ChIP analysis was carried out. The ChIP assays revealed that ANRIL knockdown reduced the binding of EZH2 to the promoters of *ERRF1* as well as H3K27me3 levels (Figure 6I). These results indicated that EZH2 could bind directly to the promoter of *ERRF1* and then repress *ERRF1* expression directly by mediating H3K27me3 demethylation modifications.

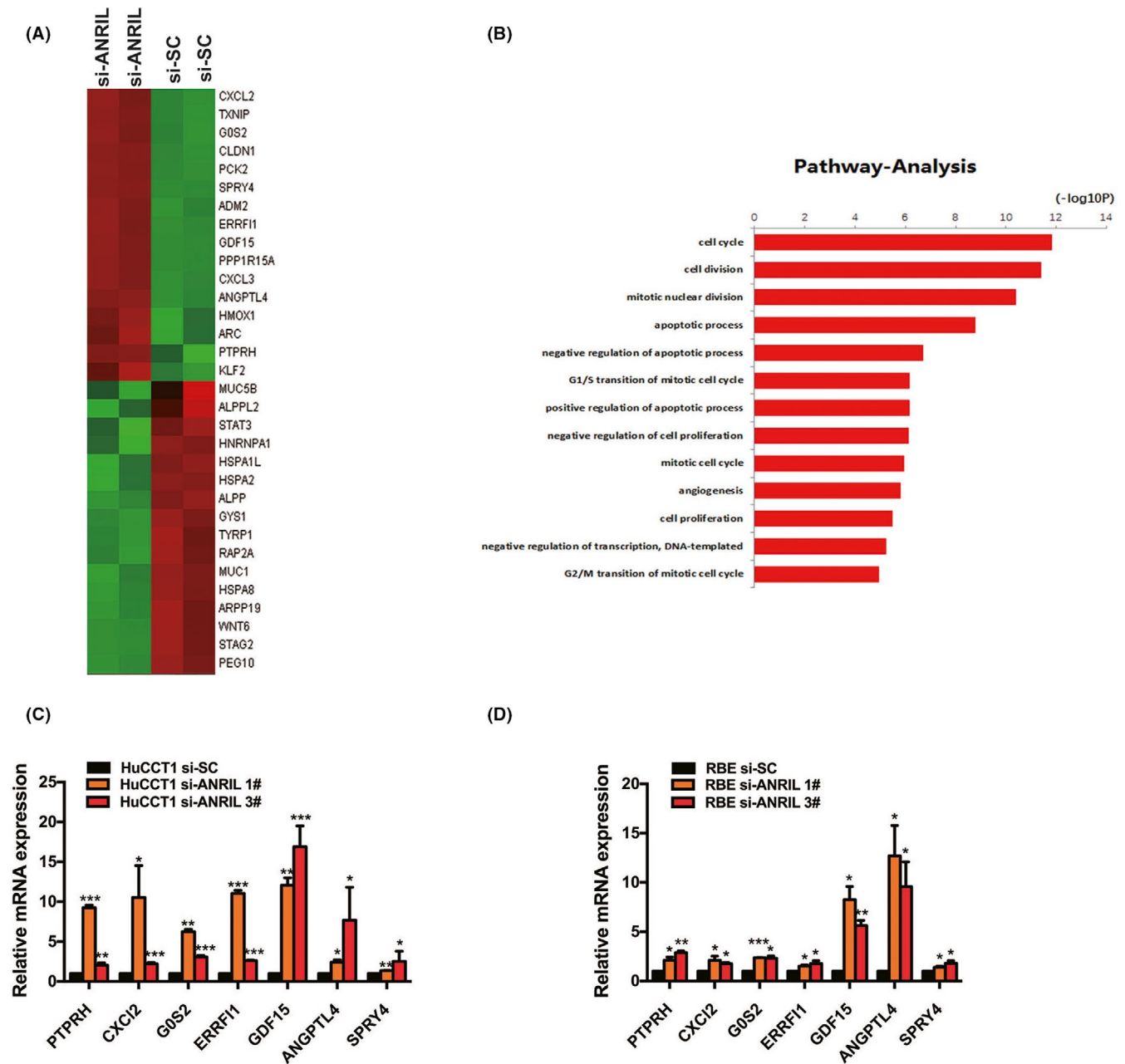


FIGURE 5 RNA sequencing after *ANRIL* knockdown in HuCCT1 cholangiocarcinoma cells. A, Mean-centered, hierarchical clustering of the 2733 transcripts altered (≥ 1.5 -fold change) in scrambled negative control siRNA (si-SC)-treated cells and siRNA-*ANRIL*-treated cells with 2 repeats. B, Gene ontology analysis for all genes with altered expression. C, D, Altered mRNA levels were selectively confirmed by quantitative RT-PCR in *ANRIL* knockdown cells. Error bars indicate means \pm SD. * $P < .05$; ** $P < .01$; *** $P < .001$

3.7 | Overexpression of *ERRF1* suppresses CCA cell proliferation and metastasis, and *ERRF1* is a confirmed target of *ANRIL*

ERRF1, also known as *Mig-6* and *RALT*, can inhibit cancer cell proliferation and migration, including in non-small cell lung cancer,^{53,54} endometrial cancer,^{55,56} hepatocellular carcinoma,^{57,58} endometrial cancer,⁵⁹ and papillary thyroid cancer.⁶⁰ In addition, hypermethylation of the *ERRF1* promoter region has been reported to contribute to *ERRF1* transcription inactivation.⁶¹ However, no report has proven that *ERRF1* is a tumor suppressor gene in CCA. Therefore,

to test this hypothesis, we first analyzed the GSE76297 dataset (92 pairs of cancer and 91 normal tissue samples) and found that *ERRF1* expression was lower in CCA tissues than in normal tissues (Figure 7A). Subsequently, we detected *ERRF1* expression and found that *ERRF1* levels were lower in CCA tumor tissues than in neighboring tissues according to qRT-PCR of a cohort of 17 pairs of CCA tumor tissues and adjacent tissues (Figure 7B). Subsequently, *ERRF1* overexpression substantially suppressed the proliferation of HuCCT1 and RBE cell lines (Figure 7C,D); moreover, *ERRF1* overexpression partially reversed *ANRIL*-mediated proliferation (Figure 7E).

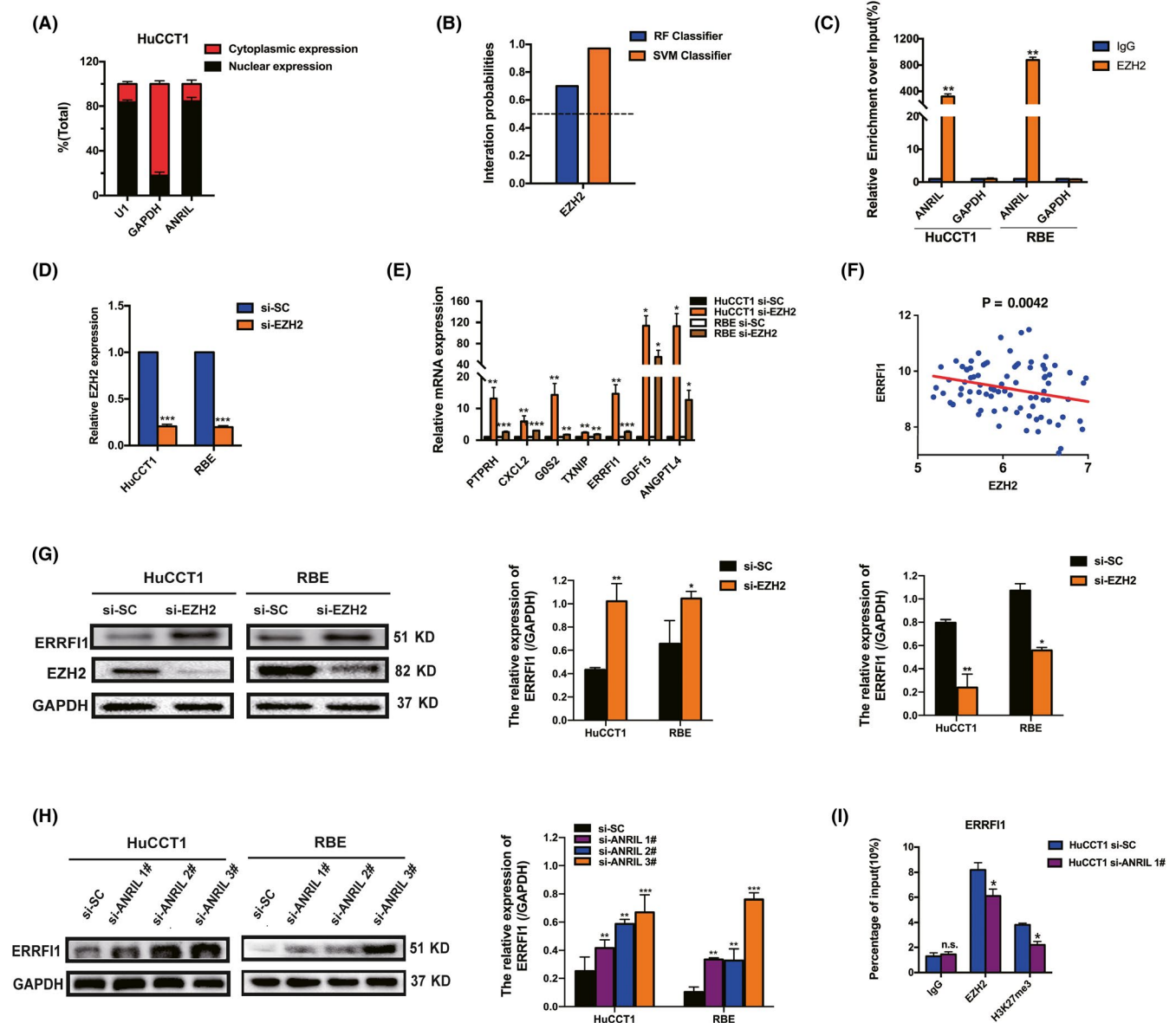


FIGURE 6 ANRIL binds to EZH2 in the nucleus to epigenetically silence *ERRF1*. A, After nuclear and cytosolic separation, RNA expression levels were measured by quantitative (q)RT-PCR. GAPDH was used as a cytosolic marker, and U1 was used as a nuclear marker. B, Interaction probabilities for EZH2 and ANRIL (<http://priddb.gdcdb.iastate.edu/RPISeq/index.html>). RF, random Forest; SVM, support vector machine. C, RIP experiments for EZH2 were carried out, and the coprecipitated RNA was subjected to qRT-PCR for ANRIL (GAPDH as the internal control). D, qRT-PCR was used to detect EZH2 expression in HuCCT1 and RBE cell lines after si-EZH2 transfection. E, Methylation-related genes were detected by qRT-PCR in HuCCT1 and RBE cell lines after EZH2 knockdown. F, Correlation between EZH2 and *ERRF1* expression was detected by analyzing GSE76297 data. G, Altered protein levels of *ERRF1* after EZH2 knockdown were selectively confirmed by western blotting. H, Altered protein levels of *ERRF1* after ANRIL knockdown were selectively confirmed by western blotting. I, ChIP-qPCR of EZH2/H3K27me3 and in *ERRF1* promoter region after transfection with scrambled negative control siRNA (si-SC) or ANRIL siRNAs in HuCCT1 cells. Enrichment was quantified with the anti-IgG Ab as an internal control. Error bars indicate means \pm SD. * $P < .05$; ** $P < .01$; *** $P < .001$; n.s., not significant

The probability of interaction between EZH2 and ANRIL was predicted on the RNA-Protein Interaction Prediction website, and the result showed that EZH2 could bind well with ANRIL. For the RIP experiment, endogenous ANRIL was amplified in the anti-EZH2 RIP fraction relative to the input. These results confirmed that ANRIL could interact with EZH2. In addition, ChIP assays revealed that ANRIL knockdown reduced the binding of EZH2 to the promoters of *ERRF1* as well as H3K27me3 levels, leading to increased levels of *ERRF1*, which could decelerate CCA growth (Figure 7F). In

conclusion, our results indicated that ANRIL promotes CCA malignancy by binding to EZH2 and then epigenetically repressing *ERRF1* expression in the nucleus.

4 | DISCUSSION

Recent advances in high-throughput biotechnologies have led to the exponential growth of high-resolution lncRNA profiles of specimens

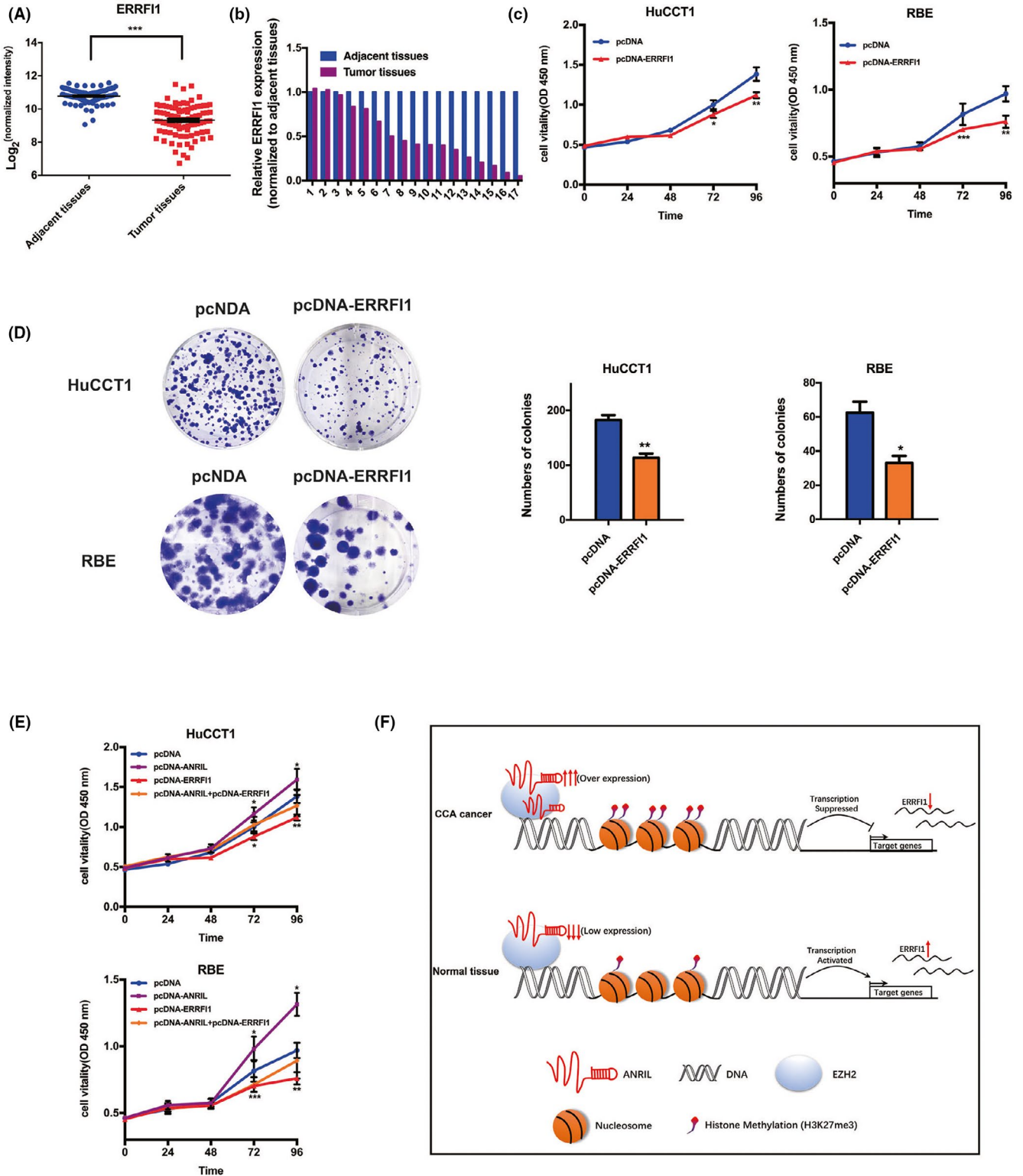


FIGURE 7 *ERRF1* overexpression suppresses cholangiocarcinoma (CCA) cell proliferation and metastasis, and *ERRF1* is a confirmed target of *ANRIL*. A, *ERRF1* expression levels in CCA according to GSE76297 data analysis. B, *ERRF1* was detected in 17 pairs of CCA tissues by quantitative RT-PCR. *ERRF1* levels were significantly lower in CCA tissues than in nontumorous tissues. C, CCK-8 assays were used to determine the cell viability of pcDNA-*ERRF1*-transfected CAA cells. D, Colony formation assays were used to determine the cell colony formation ability of pcDNA-*ERRF1*-transfected cells. E, HuCCT1 and RBE cells transfected with vector/pcDNA-*ERRF1*/pcDNA-*ANRIL* were transfected with *ANRIL* followed by *ERRF1*. After transfection, the cells were analyzed by CCK-8 assays. F, Proposed model in which *ANRIL* interacts with *EZH2* to suppress *ERRF1* expression and promote CCA tumor growth. Error bars indicate means \pm SD. * $P < .05$; ** $P < .01$; *** $P < .001$

from various types of cancer. These newly detectable lncRNAs have proven to be critical players in diverse human diseases, particularly human cancers. Research has shown that *ANRIL* levels are much higher in CCA tissues than in matched nontumor tissues. This led us to hypothesize that *ANRIL* might play a significant role in CCA malignancy. In fact, *ANRIL* has been identified as part of a shared genetic susceptibility locus associated with intracranial aneurysm,^{31,32} coronary disease,³³ and various types of cancers, particularly the invasive pathophysiology of ovarian cancer,³⁴ nasopharyngeal carcinoma,³⁵ hepatocellular carcinoma,³⁶ lung cancer,^{37,38} epithelial ovarian cancer,³⁴ colorectal cancer,^{39,40} cervical cancer,⁴¹ and gastric cancer.⁴²

We discovered that silencing *ANRIL* could inhibit CCA cell proliferation and migration in vitro and in vivo. Although *ANRIL* has been proposed to have oncogenic functions in diverse types of cancer, the global genes regulated by *ANRIL* have not been discovered. Through RNA-seq, we noted that the gene ontology analysis results were particularly related to proliferation and migration, which agreed with the prevention of proliferation and migration in CCA cell lines with *ANRIL* knockdown. Recent studies have shown that many lncRNAs cooperate with chromatin-modifying enzymes to stimulate epigenetic activation and thus silence the expression of the target genes.⁵⁰ For instance, the lncRNA *PVT1* can interact with enhancer of *EZH2*, which is needed to suppress *p15* and *p16* in gastric cancer.⁶² Moreover, lncRNAs can serve as scaffolds for protein complexes.⁶³⁻⁶⁵ For example, the lncRNA *CCAT1* can act as a scaffold for double epigenetic modification complexes (the 5'-domain of *CCAT1* binding *PRC2* with the 3'-binding domain of *SUV39H1*) and then mediate histone methylation at the promoter locus of *SPRY4* in esophageal squamous cell carcinoma.⁶⁶ Our results show that *ANRIL* could bind to *EZH2*, a type of histone methylation modification complex in the nucleus, and thus regulate the expression of a series of target genes, including *ERRF1*, a novel tumor suppressor in CCA.

In particular, previous studies have shown that *ERRF1* can act as a tumor suppressor gene in many types of cancers.⁶⁷ Nevertheless, the function of *ERRF1* in the tumorigenesis of CCA remains unknown. Our data revealed that histone methylation (H3K27me3) modulated by *ANRIL* could facilitate the lower expression of *ERRF1* in CCA cell lines. In combination with these findings, the functional interaction between *ANRIL* and *EZH2* that we characterized in this study further emphasizes the centrality of lncRNAs in regulating gene expression, including that of *ERRF1*, a novel tumor suppressor. Our results also suggest that interaction with chromatin-modifying complexes is an important mechanism by which *ANRIL* exerts its functions in CCA.

In summary, our study revealed the regulatory mechanism of *ANRIL* in tumorigenesis. *ANRIL* promotes CCA malignancy through epigenetically regulating *ERRF1* transcription in the nucleus, thus facilitating cell survival and metastasis in CCA. To this end, rapid advances in oligonucleotide/nanoparticle technology support the development of siRNA-based therapeutics to regulate lncRNA levels in vivo. In light of our findings, further investigation into the potential of *ANRIL* as an informative biomarker and therapeutic target for patients with CCA is warranted.

ACKNOWLEDGMENTS

This study was supported by the Project of Standard Diagnosis and Treatment of Key Disease of Jiangsu Province (BE2015722), the Project of the Peak of the Six Talents of Jiangsu Province (WSN-018), and the Scientific Research Foundation for Health of Jiangsu Province (H201408). We also thank NovelBio Bio-Pharm Technology Co., Ltd. for their support of the next-generation sequencing and bioinformatics analysis with the NovelBrain Cloud Analysis Platform (www.novelbrain.com)

CONFLICT OF INTEREST

None.

ORCID

Qiaoyu Chen  <https://orcid.org/0000-0001-5979-5088>

Lin Miao  <https://orcid.org/0000-0002-1114-0530>

REFERENCES

1. Wang W-T, Ye H, Wei P-P, et al. LncRNAs H19 and HULC, activated by oxidative stress, promote cell migration and invasion in cholangiocarcinoma through a ceRNA manner. *J Hematol Oncol.* 2016;9:117.
2. Rizvi S, Borad MJ, Patel T, Gores GJ. Cholangiocarcinoma: molecular pathways and therapeutic opportunities. *Semin Liver Dis.* 2014;34:456-464.
3. Rizvi S, Gores GJ. Emerging molecular therapeutic targets for cholangiocarcinoma. *J Hepatol.* 2017;67:632-644.
4. Rizvi S, Gores GJ. Pathogenesis, diagnosis, and management of cholangiocarcinoma. *Gastroenterology.* 2013;145:1215-1229.
5. Zhu AX. Future directions in the treatment of cholangiocarcinoma. *Best Pract Res Clin Gastroenterol.* 2015;29:355-361.
6. Valle J, Wasan H, Palmer DH, et al. Cisplatin plus gemcitabine versus gemcitabine for biliary tract cancer. *N Engl J Med.* 2010;362:1273-1281.
7. Lee S, Kopp F, Chang T-C, et al. Noncoding RNA NORAD regulates genomic stability by sequestering PUMILIO proteins. *Cell.* 2016;164:69-80.
8. Niazi F, Valadkhan S. Computational analysis of functional long noncoding RNAs reveals lack of peptide-coding capacity and parallels with 3'UTRs. *RNA.* 2012;18:825-843.
9. Zhao J, Liu Y, Zhang W, et al. Long non-coding RNA Linc00152 is involved in cell cycle arrest, apoptosis, epithelial to mesenchymal transition, cell migration and invasion in gastric cancer. *Cell Cycle.* 2015;14:3112-3123.
10. Jia H, Osak M, Bogu GK, Stanton LW, Johnson R, Lipovich L. Genome-wide computational identification and manual annotation of human long noncoding RNA genes. *RNA.* 2010;16:1478-1487.
11. Saha A, Bhattacharya S, Bhattacharya A. Serum stress responsive gene EhsLncRNA of *Entamoeba histolytica* is a novel long noncoding RNA. *Sci Rep.* 2016;6:27476.
12. Kugel JF, Goodrich JA. Non-coding RNAs: key regulators of mammalian transcription. *Trends Biochem Sci.* 2012;37:144-151.
13. Hu X, Feng YI, Zhang D, et al. A functional genomic approach identifies *FAL1* as an oncogenic long noncoding RNA that associates with *BMI1* and represses *p21* expression in cancer. *Cancer Cell.* 2014;26:344-357.
14. Sun M, Nie F, Wang Y, et al. LncRNA *HOXA11-AS* promotes proliferation and invasion of gastric cancer by scaffolding the chromatin modification factors *PRC2*, *LSD1*, and *DNMT1*. *Cancer Res.* 2016;76:6299-6310.

15. Guttman M, Donaghey J, Carey BW, et al. lincRNAs act in the circuitry controlling pluripotency and differentiation. *Nature*. 2011;477:295-300.
16. Beckedorff FC, Amaral MS, Deocesano-Pereira C, Verjovski-Almeida S. Long non-coding RNAs and their implications in cancer epigenetics. *Biosci Rep*. 2013;33:e00061.
17. Atianand MK, Hu W, Satpathy AT, et al. A long noncoding RNA lincRNA-EPS acts as a transcriptional brake to restrain inflammation. *Cell*. 2016;165:1672-1685.
18. Simon MD, Pinter SF, Fang R, et al. High-resolution Xist binding maps reveal two-step spreading during X-chromosome inactivation. *Nature*. 2013;504:465-469.
19. Engreitz JM, Pandya-Jones A, McDonel P, et al. The Xist lncRNA exploits three-dimensional genome architecture to spread across the X chromosome. *Science*. 2013;341:1237973.
20. Yang H, Liu P, Zhang J, et al. Long noncoding RNA MIR31HG exhibits oncogenic property in pancreatic ductal adenocarcinoma and is negatively regulated by miR-193b. *Oncogene*. 2016;35:3647-3657.
21. Guttman M, Rinn JL. Modular regulatory principles of large non-coding RNAs. *Nature*. 2012;482:339-346.
22. Shi X, Sun M, Wu Y, et al. Post-transcriptional regulation of long noncoding RNAs in cancer. *Tumour Biol*. 2015;36:503-513.
23. Ma SL, Li AJ, Hu ZY, Shang FS, Wu MC. Coexpression of the carbamoylphosphate synthase 1 gene and its long noncoding RNA correlates with poor prognosis of patients with intrahepatic cholangiocarcinoma. *Mol Med Rep*. 2015;12:7915-7926.
24. Lu X, Zhou C, Li R, Deng Y, Zhao L, Zhai W. Long noncoding RNA AFAP1-AS1 promoted tumor growth and invasion in cholangiocarcinoma. *Cell Physiol Biochem*. 2017;42:222-230.
25. Jiang XM, Li ZL, Li JL, et al. LncRNA CCAT1 as the unfavorable prognostic biomarker for cholangiocarcinoma. *Eur Rev Med Pharmacol Sci*. 2017;21:1242-1247.
26. Zhang F, Wan M, Xu Y, et al. Long noncoding RNA PCAT1 regulates extrahepatic cholangiocarcinoma progression via the Wnt/beta-catenin-signaling pathway. *Biomed Pharmacother*. 2017;94:55-62.
27. Tan X, Huang Z, Li X. Long non-coding RNA MALAT1 interacts with miR-204 to modulate human hilar cholangiocarcinoma proliferation, migration, and invasion by targeting CXCR4. *J Cell Biochem*. 2017;118:3643-3653.
28. Wang C, Mao Z P, Wang L, et al. Long non-coding RNA MALAT1 promotes cholangiocarcinoma cell proliferation and invasion by activating PI3K/Akt pathway. *Neoplasma*. 2017;64:725-731.
29. Zhang C, Li JY, Tian FZ, et al. LncRNA NEAT1 promotes growth and metastasis of cholangiocarcinoma cells. *Oncol Res*. 2017;26:879-888.
30. Zhang S, Xiao J, Chai Y, et al. LncRNA-CCAT1 promotes migration, invasion, and EMT in intrahepatic cholangiocarcinoma through suppressing miR-152. *Dig Dis Sci*. 2017;62:3050-3058.
31. Che J. Molecular mechanisms of the intracranial aneurysms and their association with the long noncoding ribonucleic acid ANRIL - a review of literature. *Neurol India*. 2017;65:718-728.
32. Foroud T, Koller DL, Lai D, et al. Genome-wide association study of intracranial aneurysms confirms role of Anril and SOX17 in disease risk. *Stroke*. 2012;43:2846-2852.
33. Zhuang J, Peng W, Li H, et al. Methylation of p15INK4b and expression of ANRIL on chromosome 9p21 are associated with coronary artery disease. *PLoS ONE*. 2012;7:e47193.
34. Qiu JJ, Wang Y, Liu YL, Zhang Y, Ding JX, Hua KQ. The long non-coding RNA ANRIL promotes proliferation and cell cycle progression and inhibits apoptosis and senescence in epithelial ovarian cancer. *Oncotarget*. 2016;7:32478-32492.
35. Hu X, Jiang H, Jiang X. Downregulation of lncRNA ANRIL inhibits proliferation, induces apoptosis, and enhances radiosensitivity in nasopharyngeal carcinoma cells through regulating miR-125a. *Cancer Biol Ther*. 2017;18:331-338.
36. Hua L, Wang CY, Yao KH, Chen JT, Zhang JJ, Ma WL. High expression of long non-coding RNA ANRIL is associated with poor prognosis in hepatocellular carcinoma. *Int J Clin Exp Pathol*. 2015;8:3076-3082.
37. Lin L, Gu ZT, Chen WH, Cao KJ. Increased expression of the long non-coding RNA ANRIL promotes lung cancer cell metastasis and correlates with poor prognosis. *Diagn Pathol*. 2015;10:14.
38. Nie F-Q, Sun M, Yang J-S, et al. Long noncoding RNA ANRIL promotes non-small cell lung cancer cell proliferation and inhibits apoptosis by silencing KLF2 and P21 expression. *Mol Cancer Ther*. 2015;14:268-277.
39. Sun Z, Ou C, Ren W, Xie X, Li X, Li G. Downregulation of long non-coding RNA ANRIL suppresses lymphangiogenesis and lymphatic metastasis in colorectal cancer. *Oncotarget*. 2016;7:47536-47555.
40. Sun Y, Zheng ZP, Li H, Zhang HQ, Ma FQ. ANRIL is associated with the survival rate of patients with colorectal cancer, and affects cell migration and invasion in vitro. *Mol Med Rep*. 2016;14:1714-1720.
41. Zhang D, Sun G, Zhang H, Tian J, Li Y. Long non-coding RNA ANRIL indicates a poor prognosis of cervical cancer and promotes carcinogenesis via PI3K/Akt pathways. *Biomed Pharmacother*. 2016;85:511-516.
42. Zhang EB, Kong R, Yin DD, et al. Long noncoding RNA ANRIL indicates a poor prognosis of gastric cancer and promotes tumor growth by epigenetically silencing of miR-99a/miR-449a. *Oncotarget*. 2014;5:2276-2292.
43. Chen S, Zhang J-Q, Chen J-Z, et al. The over expression of long non-coding RNA ANRIL promotes epithelial-mesenchymal transition by activating the ATM-E2F1 signaling pathway in pancreatic cancer: an in vivo and in vitro study. *Int J Biol Macromol*. 2017;102:718-728.
44. Kotake Y, Nakagawa T, Kitagawa K, et al. Long non-coding RNA ANRIL is required for the PRC2 recruitment to and silencing of p15(INK4B) tumor suppressor gene. *Oncogene*. 2011;30:1956-1962.
45. Xu Y, Ge Z, Zhang E, et al. The lncRNA TUG1 modulates proliferation in trophoblast cells via epigenetic suppression of RND3. *Cell Death Dis*. 2017;8:e3104.
46. Zhao B, Lu YL, Yang Y, et al. Overexpression of lncRNA ANRIL promoted the proliferation and migration of prostate cancer cells via regulating let-7a/TGF-beta1/Smad signaling pathway. *Cancer Biomark*. 2018;21:613-620.
47. Mehta-Mujoo PM, Cunliffe HE, Hung NA, Slatte TL. Long non-coding RNA ANRIL in the nucleus associates with periostin expression in breast cancer. *Front Oncol*. 2019;9:885.
48. Zhuo W, Liu Y, Li S, et al. Long noncoding RNA GMAN, up-regulated in gastric cancer tissues, is associated with metastasis in patients and promotes translation of Ephrin A1 by competitively binding GMAN-AS. *Gastroenterology*. 2019;156(676-691):e611.
49. Micheletti R, Plaisance I, Abraham BJ, et al. The long noncoding RNA Wisper controls cardiac fibrosis and remodeling. *Sci Transl Med*. 2017;9:eaai9118.
50. Marchese FP, Huarte M. Long non-coding RNAs and chromatin modifiers: their place in the epigenetic code. *Epigenetics*. 2014;9:21-26.
51. Shen X, Liu Y, Hsu Y-J, et al. EZH1 mediates methylation on histone H3 lysine 27 and complements EZH2 in maintaining stem cell identity and executing pluripotency. *Mol Cell*. 2008;32:491-502.
52. Yamaguchi H, Hung MC. Regulation and role of EZH2 in cancer. *Cancer Res Treat*. 2014;46:209-222.
53. Li Z, Dong Q, Wang Y, Qu L, Qiu X, Wang E. Downregulation of Mig-6 in nonsmall-cell lung cancer is associated with EGFR signaling. *Mol Carcinog*. 2012;51:522-534.
54. Li Z, Qu L, Zhong H, Xu K, Qiu X, Wang E. Low expression of Mig-6 is associated with poor survival outcome in NSCLC and inhibits

- cell apoptosis via ERK-mediated upregulation of Bcl-2. *Oncol Rep.* 2014;31:1707-1714.
55. Kim TH, Lee D-K, Cho S-N, et al. Critical tumor suppressor function mediated by epithelial Mig-6 in endometrial cancer. *Cancer Res.* 2013;73:5090-5099.
56. Kim TH, Yoo JY, Kim HI, et al. Mig-6 suppresses endometrial cancer associated with Pten deficiency and ERK activation. *Cancer Res.* 2014;74:7371-7382.
57. Li Z, Qu L, Luo W, et al. Mig-6 is down-regulated in HCC and inhibits the proliferation of HCC cells via the P-ERK/Cyclin D1 pathway. *Exp Mol Pathol.* 2017;102:492-499.
58. Reschke M, Ferby I, Stepniak E, et al. Mitogen-inducible gene-6 is a negative regulator of epidermal growth factor receptor signaling in hepatocytes and human hepatocellular carcinoma. *Hepatology.* 2010;51:1383-1390.
59. Yoo J-Y, Yang WS, Lee JH, et al. MIG-6 negatively regulates STAT3 phosphorylation in uterine epithelial cells. *Oncogene.* 2018;37:255-262.
60. Xia T, Liao QI, Jiang X, et al. Long noncoding RNA associated-competing endogenous RNAs in gastric cancer. *Sci Rep-Uk.* 2014;4:6088.
61. Zhang YW, Staal B, Dykema KJ, Furge KA, Vande Woude GF. Cancer-type regulation of MIG-6 expression by inhibitors of methylation and histone deacetylation. *PLoS ONE.* 2012;7:e38955.
62. Kong R, Zhang E-B, Yin D-D, et al. Long noncoding RNA PVT1 indicates a poor prognosis of gastric cancer and promotes cell proliferation through epigenetically regulating p15 and p16. *Mol Cancer.* 2015;14:82.
63. Tsai M-C, Manor O, Wan Y, et al. Long noncoding RNA as modular scaffold of histone modification complexes. *Science.* 2010;329:689-693.
64. Yoon J-H, Abdelmohsen K, Kim J, et al. Scaffold function of long non-coding RNA HOTAIR in protein ubiquitination. *Nat Commun.* 2013;4:2939.
65. Puvvula PK, Desetty RD, Pineau P, et al. Long noncoding RNA PANDA and scaffold-attachment-factor SAFA control senescence entry and exit. *Nat Commun.* 2014;5:5323.
66. Zhang E, Han L, Yin D, et al. H3K27 acetylation activated-long non-coding RNA CCAT1 affects cell proliferation and migration by regulating SPRY4 and HOXB13 expression in esophageal squamous cell carcinoma. *Nucleic Acids Res.* 2017;45:3086-3101.
67. Zhang Y-W, Staal B, Su Y, et al. Evidence that MIG-6 is a tumor-suppressor gene. *Oncogene.* 2007;26:269-276.

SUPPORTING INFORMATION

Additional supporting information may be found online in the Supporting Information section.

How to cite this article: Yu Y, Chen Q, Zhang X, et al. Long noncoding RNA ANRIL promotes the malignant progression of cholangiocarcinoma by epigenetically repressing *ERRFI1* expression. *Cancer Sci.* 2020;111:2297-2309. <https://doi.org/10.1111/cas.14447>